CONSTRUCTION STATUS AND ISSUES OF THE SPALLATION NEUTRON SOURCE RING *

Jie Wei for the SNS collaboration†, Brookhaven National Laboratory, USA

Abstract

This paper presents an overview of the construction status and technical issues of the Spallation Neutron Source (SNS) accumulator ring and the transports.

DESIGN HISTORY

The SNS project is presently in the 6th year of a 7-year construction cycle [2]. The SNS ring, designed and constructed mainly by the Brookhaven National Laboratory, will accumulate pulses of 1.5×10^{14} protons of 1 GeV kinetic energy at a repetition rate of 60 Hz [1]. With a beam power of 1.5 MW in the ring, the primary concern is beam-loss induced radio-activation that can limit the ring's availability and maintainability. With a dedicated beam collimation in the ring at an efficiency above 90%, the tolerable fractional beam loss is about 10^{-3} [3].

Several key decisions were made during the period of initial R&D and the first year of construction: A study was performed comparing the present structure of full-energy linac plus accumulator ring (AR) to a rapid-cycling-synchrotron (RCS) and validated the AR design for technical feasibility and budgetary advantages [4]; A four-fold symmetric lattice was chosen to dedicate each straight section to injection, collimation, RF system, and extraction, isolating the highly radio-active collimation section from the rest for special maintenance handling; The injection was located at a dispersion-free region that allows independently adjustable painting in the transverse (with orbit bumps in the ring) and longitudinal (with an energy-spreading phase-modulated RF cavity in the HEBT) directions; A matched, "hybrid" lattice was adopted combining the FODO structure's simplicity and ease of correction with the doublet structure's flexibility for injection tuning and collimation tuning; Chromatic sextupoles and energy correction/painting cavities were base-lined for high-power operations [5]; Space was reserved and most magnets and power supplies were made compatible with future operation at upgraded energy (1.3 GeV) and power (beyond 1.5 MW). The main parameters were finalized since 2000.

Table 1: Major parameters of the SNS ring and transport.

Ring circumference	248.0 m
HEBT, RTBT length	169, 151 m
Proton beam energy	1 GeV
Average beam power	1.5 MW
Repetition rate	60 Hz
Number of protons per pulse	1.6×10^{14}
Peak RF voltage ($h=1$, 2)	(40, 20) kV
No. of RF station (ring, HEBT, RTBT)	4, 2, 0
Unnorm. emittance ($\epsilon_x+\epsilon_y$, 99%)	240 $\pi\mu$m
Betatron acceptance	480 $\pi\mu$m
RF momentum acceptance	$\pm$ 1 %
Transverse tunes (ν_x, ν_y)	6.23, 6.20
Transition energy, γ_T	5.23
No. of lattice super-periods	4
No. of dipole (ring, HEBT, RTBT)	39, 9, 1
Ring dipole field	0.7406 T
Ring dipole gap height	170 mm
No. of quad (ring, HEBT, RTBT)	53, 40, 32
Ring quad inner diameter	210-300 mm
No. of sextupole (ring, HEBT, RTBT)	20, 0, 0
Sextupole inner diameter	210-260 mm
No. of corrector (ring, HEBT, RTBT)	61, 18, 17
No. of kicker (injection, extraction)	8, 14
No. of scraper (ring, HEBT, RTBT)	4, 5, 0
No. of collimator (ring, HEBT, RTBT)	3, 3, 2
No. of vacuum pumps (ring, HEBT, RTBT)	50, 18, 12
No. of power supply (ring, HEBT, RTBT)	156, 48, 47
No. of BPM (ring, HEBT, RTBT)	44, 37, 17
No. of loss monitor (ring, HEBT, RTBT)	82, 62, 43
No. of current monitor (ring, HEBT, RTBT)	2, 5, 5
No. of profile monitor (ring, HEBT, RTBT)	4, 13, 8
Vacuum pressure (ring, HEBT, RTBT $\times10^{-8}$)	5, 1, 10 Torr

ENGINEERING STATUS & ISSUES

Magnets and power supplies

With intense design iterations (cross section, chamfers) and post-vendor retro-fitting (re-assembly, coil flipping, coil shimming), most ring magnets meet the design expectation of rms field accuracy of 10^{-4} for main dipoles and

* SNS is managed by UT-Battelle, LLC, under contract DE-AC05-00OR22725 for the U.S. Department of Energy. SNS is a partnership of six national laboratories: Argonne, Brookhaven, Jefferson, Lawrence Berkeley, Los Alamos, and Oak Ridge.

† jwei@bnl.gov

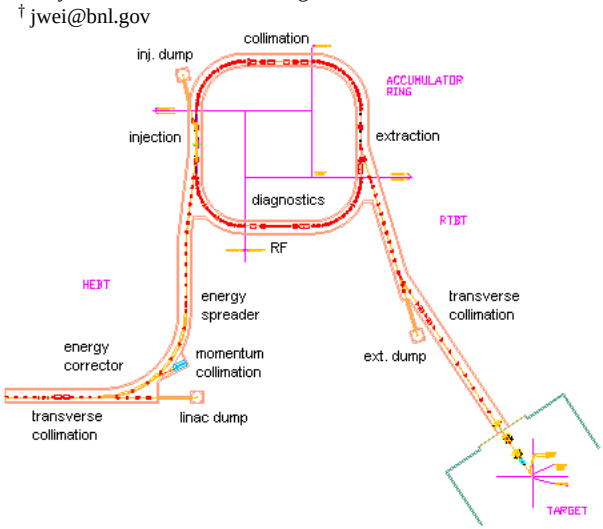

Figure 1: Layout of the SNS accumulator ring and the high energy (HEBT) and ring-to-target (RTBT) transports.

quadrupoles, 10^{-3} for sextupoles, chicane and transport magnets, and 10^{-2} for correctors at 480$\pi\mu$m acceptance ([6, 7], Table 2).

The ring dipole and quadrupole integral transfer function (ITF) are complicated by a cost-saving practice choosing solid-steel, as opposed to laminated-steel, for the magnet cores. Excessive (up to 0.25%), excitation-dependent magnet-to-magnet variations are found [7]. The magnets are shimmed with iron sheets to achieve below 10^{-4} rms variation within each power-supply family for 1 GeV operation, and sorted according to 1.3 GeV measurement data to minimize orbit corrector strength [8].

Quadrupole magnets in the straights have a narrow-body design to gain clearance for injection and extraction. Design optimization minimized lower-order multipoles, leaving a large (0.19×10^{-2}) systematic 20th pole (Table 3) whose effects are negligible during the 1 ms accumulation [10]. In case a long beam store is needed, the pole shape can be profiled to eliminate the impact of the 20th pole [9]. In addition to balancing ITF, the quadrupoles are sorted to minimize the resonance produced by the normal b_2 and skew a_2 sextupole harmonics [8].

Table 2: Measured multipoles of ring arc quadrupoles at reference radii of 80 (for 21 cm ID) and 105 mm (for 26 cm ID).

n	b_n		a_n	
	mean	S.D.	mean	S.D.
1	10000	0.00	–	–
2	−0.27	1.21	0.51	2.07
3	0.30	1.32	0.18	0.69
4	0.07	0.47	−0.05	0.45
5	1.07	0.60	−0.12	0.19
7	−0.01	0.10	−0.02	0.18
9	−0.52	0.41	0.00	0.06

Table 3: Measured multipoles of the ring 30 cm ID narrow-body quadrupoles at a reference radius of 115 mm.

n	b_n		a_n	
	mean	S.D.	mean	S.D.
1	10000	0.00	–	–
2	2.97	2.86	−0.87	1.45
3	0.04	0.70	1.31	0.37
4	0.38	0.63	−0.08	0.43
5	2.58	0.38	0.16	0.56
7	−0.01	0.08	0.06	0.08
9	−21.7	0.53	0.00	0.08

20 sextupoles grouped in four families are arranged in lattice symmetry for chromatic adjustment without lattice disruption. The reduction in quadrupole transfer function (-0.2%) caused by the interference from nearby sextupole/corrector is easily compensated [5]. The ring correction elements consist of horizontal and vertical dipoles, normal and skew quadrupoles, normal and skew sextupoles, and octupoles for orbit correction, decoupling, amplitude detuning, and resonance corrections. Octupoles can be rotated to act as skew-octupoles if needed. Resonance correction strategy is developed in the presence of space charge [10]. The multi-coil corrector design results in a large (6%) decapole in skew-sextupole correction.

There is 1 power supply for the main dipoles, 6 for the quadrupoles, 4 for the sextupoles, 115 for the correctors and chicane dipoles, 8 for the injection kickers, and 14 for the extraction kickers. Good rise/fall time and matching have been achieved on pulsed supplies (programmable injection and extraction) [11].

Injection

The 30 m long H^- injection region contains 2 pairs of lattice quadrupole doublets, 4 chicane dipoles for the DC bump, 4 horizontal and 4 vertical kickers with programmable power supplies for transverse painting, a injection dipole, and a combined-function magnet that guides both stripped H^0 and H^- beams to the 200 kW injection dump [12]. The two chicane dipoles near the stripping foil are tapered to guide the stripped electrons to the heat-resistant, low-reflection C-C collector which is attached to a water-cooled copper plate [13]. A clearing electrode near the foil can apply up to 10 kV voltage to suppress electron multipacting [14]. The two stripping foils and the electron catcher are all monitored by video systems. Free-hanging carbon and diamond foils are under development [15] for mounting on a quick-exchange mechanism.

Due to design complexion, the injection components are trial-assembled at BNL to eliminate mechanical interferences. The tapered chicane magnets are successfully measured with both a long coil for integral field compensation and a point coil for field-angle calibration. The measured kicker rise time ($\sim$175 μs) also satisfies design expectation.

Collimation & remote handling

To protect the ring for a full-energy injection, the H^- beam in HEBT is collimated transversely with 4 pairs of adjustable scraping foils spaced in 90° betatron phase along with 2 fully shielded collimators, and longitudinally at the high-dispersion location in the 90°-bend achromat.

The proton beam in the ring is cleaned transversely with a two-stage system consisting of 4 adjustable, thin tantalum scrapers spaced in 45° angles, and 3 shielded, 1.5 m long secondary collimators. The collimator vacuum chambers are made of double-layered Inconel filled with helium gas between the layers to detect leaks [16, 17]. Solenoids are wounded around connecting chambers to suppress electron-cloud multipacting. Longitudinally, a 4.5 m long beam-in-gap kicker cleans the beam residual during the last 100 turns before extraction.

Remote handling is adopted in "hot" region including injection, collimation, beam dump, and RTBT-target interface. Quick-disconnect vacuum flanges and remote water fittings allow easy access [18]. Collimator shieldings are designed for easy disassembly. The entire tunnel is equipped with cranes capable of 20 to 45 tons of load.

RF system

The ring dual-harmonic system maintains the beam gap for the function of extraction kicker while keeping the peak

beam current low [19]. The harmonic 1 and 2 cavities are interchangeable, providing a total voltage exceeding 60 kV. Integrated tests with the ferrite-loaded cavity, the tetrode power amplifier, and the RF control devices demonstrated a stable performance via the cavity In-phase/Quadruture loop and the dynamic tuning loop under simulated accumulation of a full beam intensity (frequency sweep from 1.03 to 1.21 MHz). The dynamic tuning is realized by continuously changing the ferrite bias and thus cavity resonance frequency, reducing the RF drive current.

Extraction

The kicker system consists of 14 individually powered modules, so that beam loss is negligible when one module fails. The pulse-forming network (PFN) units are installed outside the ring tunnel for easy maintenance. The phase advance between the extraction kicker and the target is chosen so that the beam's position on target does not change if errors develop with the kickers.

To avoid complications due to rapid variations of the magnetic field, kicker magnets are made with a single-turn coil-winding and are placed inside the vacuum chamber. Good field quality is achieved with a high-permeability ferrite material. Saturable inductors isolate the influence of the PFN, shorten the rise time ($< 0.2\mu$s), and improve the flatness of the kicker-pulse's waveform ($< 1\%$).

Extraction kickers residing inside the vacuum chamber are major sources of transverse beam-coupling impedance. The impedance associated with the high-μ ferrite was reduced by terminating the PFN circuit to 25 Ω, and by maximizing the width of the kicker [20]. Coaxial shield on the terminating resistor reduces cable reflection [21].

Vacuum and chamber coating

The design vacuum pressure is $(0.5 \sim 1)\times 10^{-7}$ Torr in HEBT to minimize H^- stripping, 10^{-8} in the ring to minimize gas scattering and ion- and electron-induced desorption, and $(0.5 \sim 1)\times 10^{-7}$ Torr in RTBT. Vacuum chambers are mostly made of stainless steel. Bellows and collimation chambers are made of Inconel to reduce radiation-induced stress corrosion. Extra pump ports are available for beam scrubbing and for future upgrades.

The inner surface of ring vacuum chamber and extraction kicker ferrite is coated with TiN. Two layers of coating are applied to the ceramic chamber for injection kickers: a 1μm-thick copper layer for by-passing the image charge, and a 0.1μm-thick TiN layer for a low electron secondary-emission yield, along with an exterior metal enclosure for dc current by-pass. This design allows the image-current passage above the lowest betatron sideband ($\sim$200 kHz) without degrading the magnetic-field penetration, eddy-current heating, and beam-induced heating. TiN coating on the ferrite of the extraction kickers is divided into 10 (V) $\times$ 50 (L) mm^2 stripes with 1 mm gaps to reduce eddy-current effects on the kicker rise time [22]. A 15 mm wide gap is also reserved around the high-voltage busses to prevent shorts through coating. TiN coating on $\sim 90\%$ ferrite surface is expected to suppresses the electron-cloud density by one order of magnitude.

Diagnostics & instrumentation

Critical devices (position monitor, loss monitor, current monitors) have been successfully demonstrated in the SNS linac beam commissioning. Fabrication of beam-line devices of all other systems (foil/catcher video monitor, wire scanner, beam-in-gap kicker, ionization profile monitor, coherent/incoherent dipole/quadrupole-mode tune systems, electron detector, and wideband dampers) is underway [23]. Extensive R&D efforts are made to improve system (e.g. IPM) performance in high-intensity operations.

Infrastructure

Intense communication is key in infrastructure parameter matching including global coordinates, device dimension and headroom, access doorways, crane clearance and capacity, "clean" power and utility power, ground breaks, cooling water volume and pressure, and operational temperature and resistance dependence [24].

SUMMARY

Construction of the SNS ring and transport is progressing as planned towards its completion in 2005. The ring complex is designed and fabricated with the potential to reach a beam energy up to 1.3 GeV and a power beyond 1.5 MW. Space is reserved for two additional extraction kickers, and for the replacement of 2 injection-chicane dipoles to minimize H^0 stripping loss. Beam instrumentation is capable of meeting the challenge of a next-generation, high-intensity accelerator complex.

We are indebted to the SNS teams and our collaborators for their devotion and contributions.

REFERENCES

[1] J. Wei, D.T. Abell, J. Beebe-Wang, et al, PRST-AB, **3** (1999) 080101; J. Wei, Rev. Mod. Phys. **75** (2003) 1383
[2] N. Holtkamp, PAC 2003, p. 11
[3] N. Catalan-Lasheras et al PRST-AB **4** (2001) 010101
[4] J. Wei, J. Beebe-Wang, et al, EPAC 2000, p. 981
[5] Y. Papaphilippou, C.J. Gardner, et al, PAC 2001 p. 1670
[6] J. Tuozzolo, J. Alduino, S.V. Badea et al, PAC 2003, p. 2156
[7] P. Wanderer, J. Jackson, A. Jain et al, PAC 2003, p. 2159
[8] D. Raparia, A. Fedotov, Y.Y. Lee, et al, these proceedings
[9] N. Tsoupas, J. Jackson, Y.Y. Lee et al, PAC 2003, p. 2153
[10] A. Fedotov, G. Parzen, PAC 2003, p. 2589
[11] R. Lambiase, J. Mi, T. Nehring et al, PAC 2001, p. 3714
[12] C. Pai, et al, these proceedings
[13] D. Abell, Y.Y. Lee, W. Meng, EPAC 2000, p. 581
[14] L. Wang, D. Raparia, J. Wei, S.Y. Zhang, these proceedings
[15] R. Shaw, R. Cutler, A.D. Herr, Y.Y. Lee et al, PAC 2003, 617
[16] H. Ludewig, J. Brodowski et al PAC 2003, p. 1428
[17] N. Simos, N. Catalan-Lasheras et al, PAC 2001, p. 1405
[18] G. Murdoch, et al, HALO'03, AIP 693 (2003), p. 172
[19] A. Zaltsman et al.; K. Smith et al, PAC 2003, p. 1195, 3344
[20] D. Davino, H. Hahn, Y.Y. Lee, EPAC 2002, p. 1467
[21] A. Zhang, J. Sandberg et al, these proceedings
[22] H. Hseuh, P. He, M. Mapes, R. Todd et al, ECLOUD 2004
[23] P. Cameron, J. Brodowski et al PAC 2003, p. 2444
[24] W. McGahern, et al, these proceedings